npj | biofilms and microbiomes

Article

Published in partnership with Nanyang Technological University

https://doi.org/10.1038/s41522-025-00812-9

Mesaconic acid as a key metabolite with anti-inflammatory and anti-aging properties produced by *Lactobacillus plantarum* 124 from centenarian gut microbiota

Lei Wu[1,2,5], Hongxin He[3,5], Tingting Liang[2,5], Guowei Du[1,5], Longyan Li[2,5], Haojie Zhong[1,5], Ying Li[2], Jinke Zhang[2], Ning Chen[2], Tong Jiang[2], Juan Yang[2], Jiangyan Wang[1], Shuo Feng[1], Shenghua Lu[1], Hui Zhao[2], Qihui Gu[2], He Gao[2], Guanghui Li[4], Wenrui Xie[1], Lihao Wu[1], Qingping Wu[2] ✉, Xinqiang Xie[1,2] ✉ & Xingxiang He[1] ✉

The gut microbiota of centenarians plays a vital role in promoting healthy longevity. We performed a cross-sectional study of 224 people from Jiaoling, China, which is globally recognised for the longevity of its residents. Compared with younger people, centenarians showed significantly increased alpha-diversity, enrichment of the beneficial bacteria *Lactobacillus*, *Akkermansia*, and *Christensenella*, and increased redox capacity in the gut microbiota. Serum metabolomics of centenarians showed significant enrichment of antioxidant metabolites, including L-ascorbic acid 2-sulphate and lipoic acid. Finally, we isolated and screened a strain of *Lactobacillus plantarum* 124 (LP124) with a good antioxidant effect on the gut microbiota of centenarians. Animal experiments further verified that mesaconic acid from LP124 regulates the gut microbiota, is anti-inflammatory, relieves oxidative stress, maintains the intestinal barrier, and is the best-known anti-aging molecule. LP124 derived from the gut microbiota of centenarians and its metabolite mesaconic acid, have a significant positive effect on health and longevity.

Aging of the global population is becoming a serious problem. Evidence exists that human gut microbiota plays a key role in human health and chronic diseases[1,2]. Therefore, the gut microbiota is an important factor in promoting human health[3,4]. Evidence from an increasing number of studies suggests that gut microbiota disorders are key factors that lead to aging and chronic disease[5–7], and that the steady state of the gut microbiota is a healthy aging regulator[8–14]. Therefore, the reconstruction of gut microbiota homoeostasis may be an important target for improving health and longevity.

Centenarians provide a good natural model for studying longevity and aging. The composition of microbiota in centenarians plays an important role in healthy aging. Multiple cross-sectional studies have shown that as people age, their microbiota shows diverse changes compared with younger controls, with fewer beneficial microbes and more opportunistic disease-causing microbes[15,16]. However, the core microbiota composition is reduced in centenarians and health-related bacteria (including *Lactobacillus*) are enriched[17]. In addition, locus cohort studies of people of different age groups

[1]Department of Gastroenterology, Research Center for Engineering Techniques of Microbiota-Targeted Therapies of Guangdong Province, The First Affiliated Hospital of Guangdong Pharmaceutical University, Guangzhou, China. [2]Guangdong Provincial Key Laboratory of Microbial Safety and Health, State Key Laboratory of Applied Microbiology Southern China, Institute of Microbiology, Guangdong Academy of Sciences, Guangzhou, China. [3]Sun Yat-sen University School of Medicine, Guangzhou, China. [4]College of Light Industry and Food Technology, Guangdong Provincial Key Laboratory of Lingnan Specialty Food Science and Technology, Academy of Contemporary Agricultural Engineering Innovations, Zhongkai University of Agriculture and Engineering, Guangzhou, China. [5]These authors contributed equally: Lei Wu, Hongxin He, Tingting Liang, Guowei Du, Longyan Li, Haojie Zhong. ✉e-mail: wuqp203@163.com; woshixinqiang@126.com; hexingxiang@gdpu.edu.cn

and population locations have shown that novel bile acid biosynthesis pathways are abundant in the microbiota of centenarians and that the gut microbiota of centenarians has an exogenous material degradation function[18,19]. Longevity-related gut microbiota (such as *Christensenellaceae*, *Porphyromonadaceae* and *Rikenellaceae*) and functions (such as xenobiotic degradation) play important roles in healthy longevity[18–23]. Although these studies established an association between gut microbiota and longevity, they lacked further responses to these findings. Key beneficial or detrimental strains were not isolated, identified, preserved, and screened. Furthermore, the anti-aging function of key strains was not verified in vitro and in vivo. Finally, the key substance for the anti-aging effect of key strains was not determined and verified. Therefore, more detailed comparisons, larger sample sizes, longer trajectories, and further strain isolation screening and validation are needed to determine the function of the microbiome in centenarians and anti-aging measures to clarify the relationship between gut microbiota and health and longevity.

Previously, we observed that the gut microbiota of long-lived individuals contained a high abundance of health-related *Lactobacillus*[7]. In this regard, we targeted the isolation of *Lactobacillus* in the gut microbiota of a long-lived township population and screened and verified *Lactobacillus plantarum* 124 (LP124) with good anti-aging function through in vitro screening and in vivo verification methods. Metabolomics analysis showed that the serum levels of mesoconic acid (MA), lysine (Lys), and butyrate (But) in mice administered with LP124 were significantly higher than those in the model group. To explore the potential anti-aging role of LP124, we studied the anti-inflammatory and anti-aging effects of MA, Lys, and But on the aging process.

We performed a cross-sectional study involving 224 participants that included centenarians and other age groups (20–110 years). We examined the gut microbiota structure and function of all participants using metagenome analysis and characterised the serum differential metabolites of all participants using metabolome analysis. Based on our previous results, we further verified the anti-inflammatory and anti-aging effects of mesaconic acid, lysine, and butyrate on the metabolites of *Lactobacillus plantarum* 124 (LP124), a longevity-related strain, through animal experiments. This study aimed to explore that gut microbiota, especially gut probiotics and their metabolites, have a positive effect on health and longevity in long-lived people.

Results

Composition and functional characteristics of gut microbiota in long-lived people of different ages

According to age, the population in the long-lived areas was divided into middle-aged (Y40: 21–40 years and Y60: 41–60 years), older adults (Y80: 61–80 years and Y100: 81–99 years), and centenarian (Y120: 100–110 years) groups. The top 35 relative abundance of the gut microbiota at the genus level were shown in Fig. 1A. Principal component analysis (PCA) identified two of the most variable classes across all populations, *Bacteroides* and *Parabacteroides*, which are major contributors to the human gut type (Fig. 1B). A constructed taxonomic phylogenetic tree showed that the genera level species abundance of the Y40, Y60, Y80, and Y100 groups differed significantly from that of the Y120 group ($P < 0.05$). Summarising the species selected by comparing Y40 vs. Y120, Y60 vs. Y120, Y80 vs. Y120, and Y100 vs. Y120 groups identified 281 distinct species (Fig. 1C). Diversity characteristics of the gut microbiota in long-lived people of different ages were examined. According to Chao1 index values, the gut microbiota diversity of the centenarian group (Y120) was significantly higher than that of the middle-aged groups (Y40 and Y60) (Fig. 2A–D). Principal coordinates analysis (PCoA) showed that the gut microbiota of the centenarian group (Y120) was different from the middle-aged (Y40, Y60) and the older adult (Y80, Y100) groups (Fig. 2E–H). A volcano map of the different bacteria was drawn according to the *P*-values of the DESeq2 analysis results. The beneficial bacteria *Akkermansia*, *Lactobacillus*, and *Christensenella* in the gut microbiota of the centenarian group (Y120) were significantly more prevalent than those in the middle-aged (Y40, Y60) and older adult (Y100) groups (Fig. 2I–L). The findings indicate that these beneficial bacteria play important roles in health and longevity.

To explore the role of the beneficial bacteria *Akkermansia*, *Lactobacillus*, and *Christensenella* in health and longevity, we screened 281 distinct species with an abundance $>10^{-5}$. Spearman correlation analysis was performed for the Y40, Y60, Y80, Y100, and Y120 groups. The *Akkermansia*, *Lactobacillus*, and *Christensenella* genera correlated with absolute correlation coefficient values > 0.4 were presented at network and heat maps (Fig. 3). *Akkermansia* strongly correlated with *Acholeplasma*, *Brevibacillus*, *Caloramator*, and other genera in the Y120 group (Fig. 3A–F). *Christensenella* was strongly correlated with *Massilimaliae*, *Provencibacterium*, and *Ruminiclostridium*, in the Y40, Y60, Y80, Y100, and Y120 groups (Fig. 3A–E, G). *Lactobacillus* strongly correlated with *Acholeplasma*, *Criibacterium*, *Desulfotomaculum*, *Lachnobacterium*, and other genera in the Y120 group (Fig. 3A–E, H). Analysis of metabolic pathways revealed changes in gene abundance (Fig. 4). In the functional genes pathway with the largest difference in abundance, the abundance of related genes in the Y100 and Y120 groups was significantly higher than that in the Y40, Y60, and Y80 groups. The microbiota of centenarians showed a significantly increased redox capacity for methyltransferases, dehydrogenases, and oxidoreductases.

Serum metabolomics characteristics of longevity population at different ages

We further characterised the serum metabolomics of the different age groups in the long-lived townships. Compared with the middle-aged (Y40, Y60) and older adult (Y80, Y100) groups, the relative expression levels of the L-ascorbic acid 2-sulphate, (R)-lipoic acid, L-arginine, lipoamide, fumaric acid, citraconic acid, glutamine, ascorbic acid, and taurolithocholic acid 3-sulphate metabolites were higher in the centenarian group (Y120) under the negative mode (Supplementary Fig. 1). The relative expression levels of the indole-3-butyric acid, glycochenodeoxycholic acid, methionine sulfoxide, dehydrocholic acid, glycocholic acid, arachidonoyl amide, and 5-hydroxyindole-3-acetic acid metabolites were higher in the Y120 group in the positive mode (Supplementary Fig. 2). The findings indicate that these metabolites play important roles in health and longevity.

The analysis of differential serum metabolite characteristics between the middle-aged (Y40, Y60), older adult (Y80, Y100), and centenarian (Y120) groups is shown in Fig. 5. Glutamine, taurolithocholic acid 3-sulphate, glycochenodeoxycholic acid, fumaric acid, indole-3-butyric acid, Dl-indole-3-lactic acid, and ascorbic acid was significantly upregulated in the centenarian group (Y120) compared to the other groups. Assessment of the characteristics of the serum metabolomic Kyoto Encyclopedia of Genes and Genomes (KEGG) enrichment pathways in the different age groups revealed significant differences between the middle-aged (Y40 and Y60), older adult (Y80 and Y100), and centenarian (Y120) groups (Supplementary Fig. 3). Significantly different KEGG enrichment pathways included ascorbate and aldarate metabolism, bile secretion, citric acid (TCA) cycle, ferroptosis, glutathione metabolism, hypoxia-inducible factor-1 (HIF-1) signalling pathway, vitamin digestion and absorption, and others.

Correlation analysis of gut microbiota and serum metabolome in longevity population at different ages

We selected the top five differentially bacteria at the genus level and compared the top ten differentially expressed metabolites to analyse the correlation between the gut microbiota and metabolites. In the Y40 vs. Y120 analysis in the negative mode (Supplementary Fig. 4A), *Syntrophobotulus* was significantly and positively correlated with glutamine levels. In the Y40 vs. Y120 analysis in the positive mode (Supplementary Fig. 4B), *Alistipes* and *Desulfuromonas* were significantly positively correlated with N3,N4-dimethyl-L-arginine. *Marispirochaeta* and *Syntrophobotulus* were significantly positively correlated with glycochenodeoxycholic acid. In the Y60 vs. Y120 analysis in the negative mode (Supplementary Fig. 4C), *Methylomicrobium* was significantly positively correlated with gluconic acid. In the Y60 vs. Y120 analysis in the positive mode (Supplementary Fig. 4D),

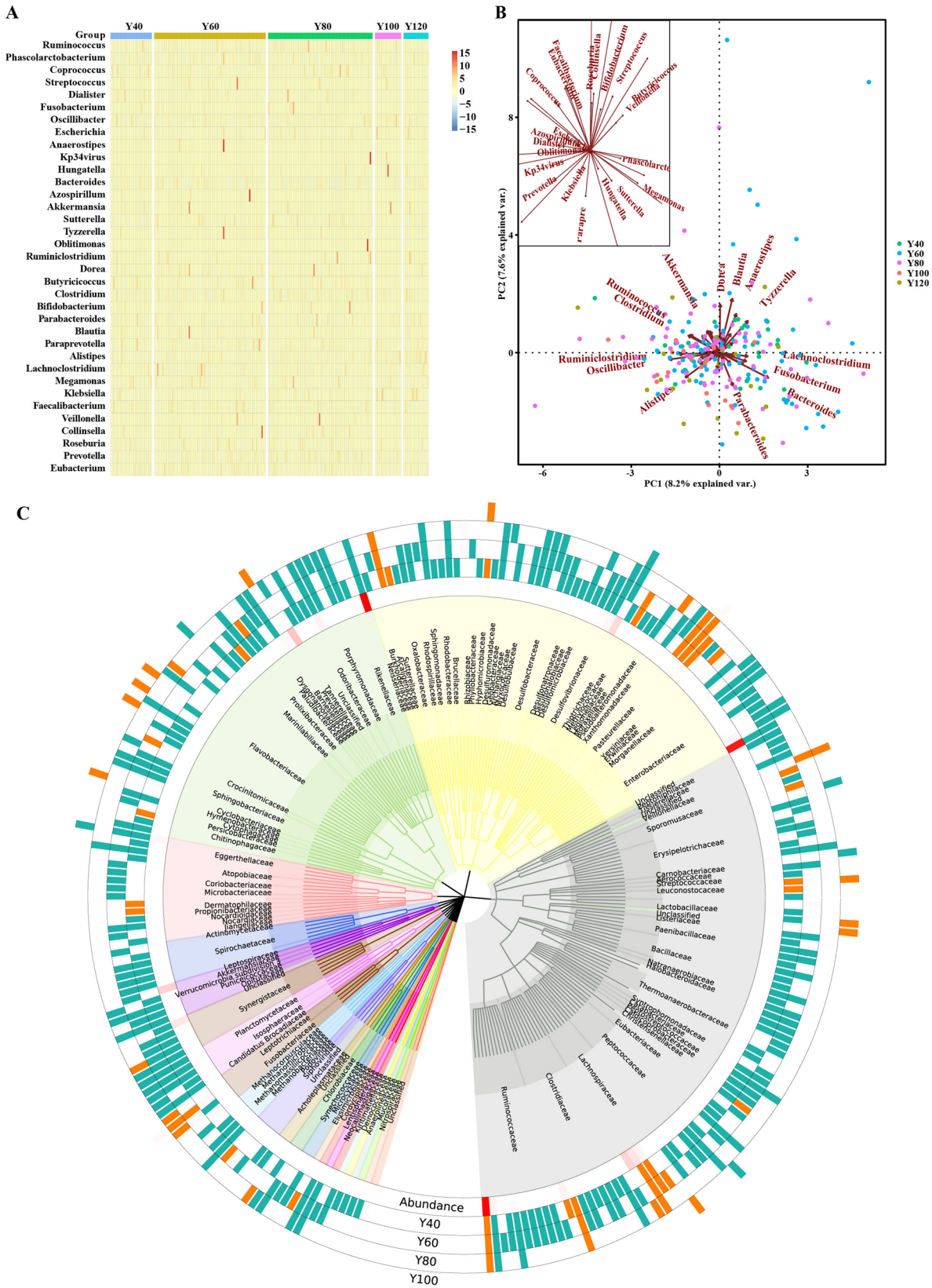

Fig. 1 | Distribution characteristics of gut microbiota in long-lived people at different ages. A Relative abundance heat map of the top 35 species at the genus level. **B** PCA map of the relative abundance level of the top 35 bacteria. PC, principal component. **C** Taxonomic phylogenetic tree for the difference analysis between the Y40, Y60, Y80, Y100, and Y120 groups. A total of 257 species from 24 phyla were selected based on 281 species, with an average relative abundance >10^{-6}. The outer ring colour indicates that the species in each group had a significant increase (orange) or decrease (green) compared with the Y120 group. The inner ring shows the mean relative abundance of each species in all samples.

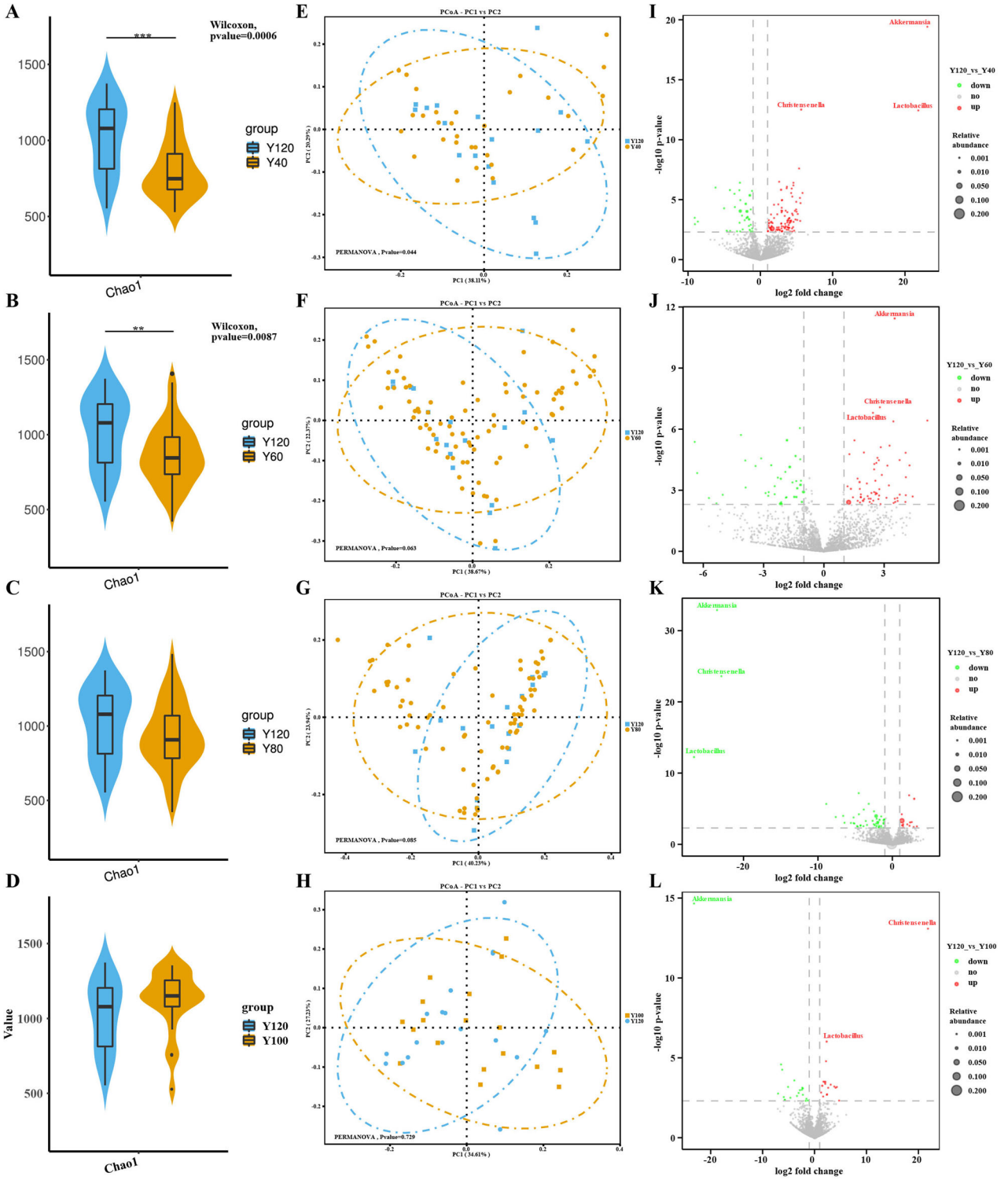

Fig. 2 | Diversity characteristics of gut microbiota in long-lived people at different ages. A–D α-diversity analysis of Y40, Y60, Y80, Y100 and Y120 groups. **E–H** PCoA of the Y40, Y60, Y80, Y100, and Y120 groups. **I–L** Volcanic map of the Y40, Y60, Y80, Y100, and Y120 groups.

Methanopyrus was significantly positively correlated with coenzyme Q2. In the Y80 vs. Y120 analysis in the negative mode (Supplementary Fig. 4E), *Bordetella, Dechloromonas, Eikenella, Holospora*, and *Leminorella* were all associated with 3-indoxyl sulphate, whereas D-(-) -ribose, D-arabinose, gluconic acid, and glutamine were negatively correlated. In the Y80 vs. Y120 analysis in the positive mode (Supplementary Fig. 4F), *Bordetella, Dechloromonas, Eikenella, Holospora*, and *Leminorella* were negatively correlated with glycodeoxycholic acid, N3, N4-dimethyl-L-arginine, and proline-hydroxyproline. In the Y100 vs. Y120 analysis in the negative mode (Supplementary Fig. 4G), *Cyclobacterium* was significantly positively correlated with 1-methyladenosine, *Slackia* negatively correlated with glyoxylate levels, and *Xanthomonas* was positively correlated with D-arabinose and taurolithocholic acid 3-sulphate. Finally, in the Y100 vs. Y120 analysis in the positive mode (Supplementary Fig. 4H), *Salegentibacter* was significantly and positively correlated with indole-3-butyric acid, and *Xanthomonas* positively correlated with glycochenodeoxycholic acid content.

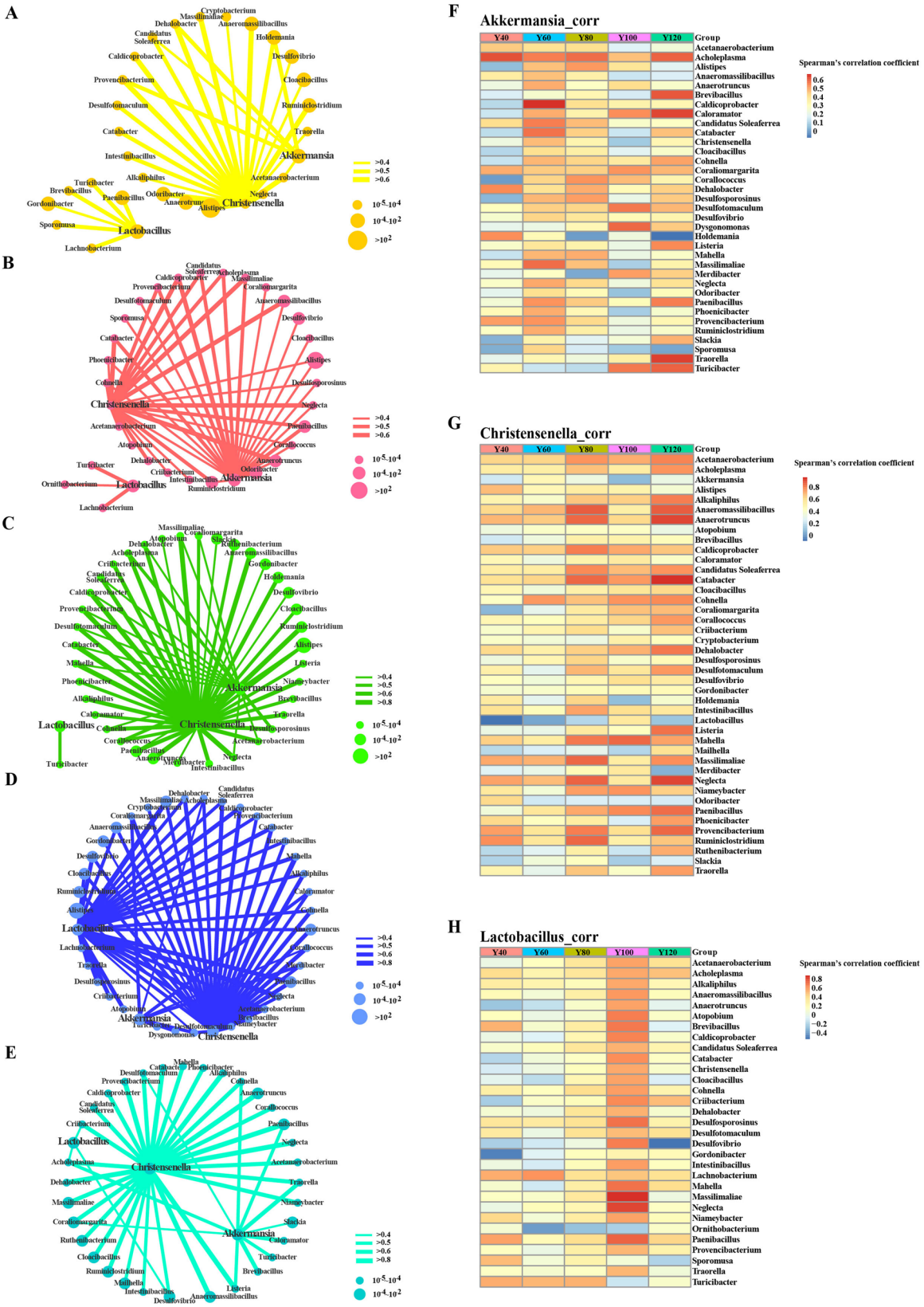

Fig. 3 | Interaction characteristics of *Akkermansia*, *Lactobacillus*, and *Christensenella* in the gut microbiota of long-lived people at different ages. A–E Interactions between *Akkermansia*, *Lactobacillus*, and *Christensenella* in the Y40, Y60, Y80, Y100, and Y120 groups. The node size is proportional to the abundance of the genus, and the line segment width is proportional to the correlation strength. **F** Correlation analysis of *Akkermansia* in the Y40, Y60, Y80, Y100, and Y120 groups. **G** Correlation analysis of *Christensenella* abundance in the Y40, Y60, Y80, Y100, and Y120 groups. **H** Correlation analysis of *Lactobacillus* in the Y40, Y60, Y80, Y100, and Y120 groups. As *Akkermansia*, *Lactobacillus*, and *Christensenella* are mainly concerned, the species related to these three numbers (abundance $>10^{-5}$) in groups Y40, Y60, Y80, Y100, and Y120 are screened, and heat maps are drawn respectively. The mapping data are the values of correlation coefficients between each species and the three genera.

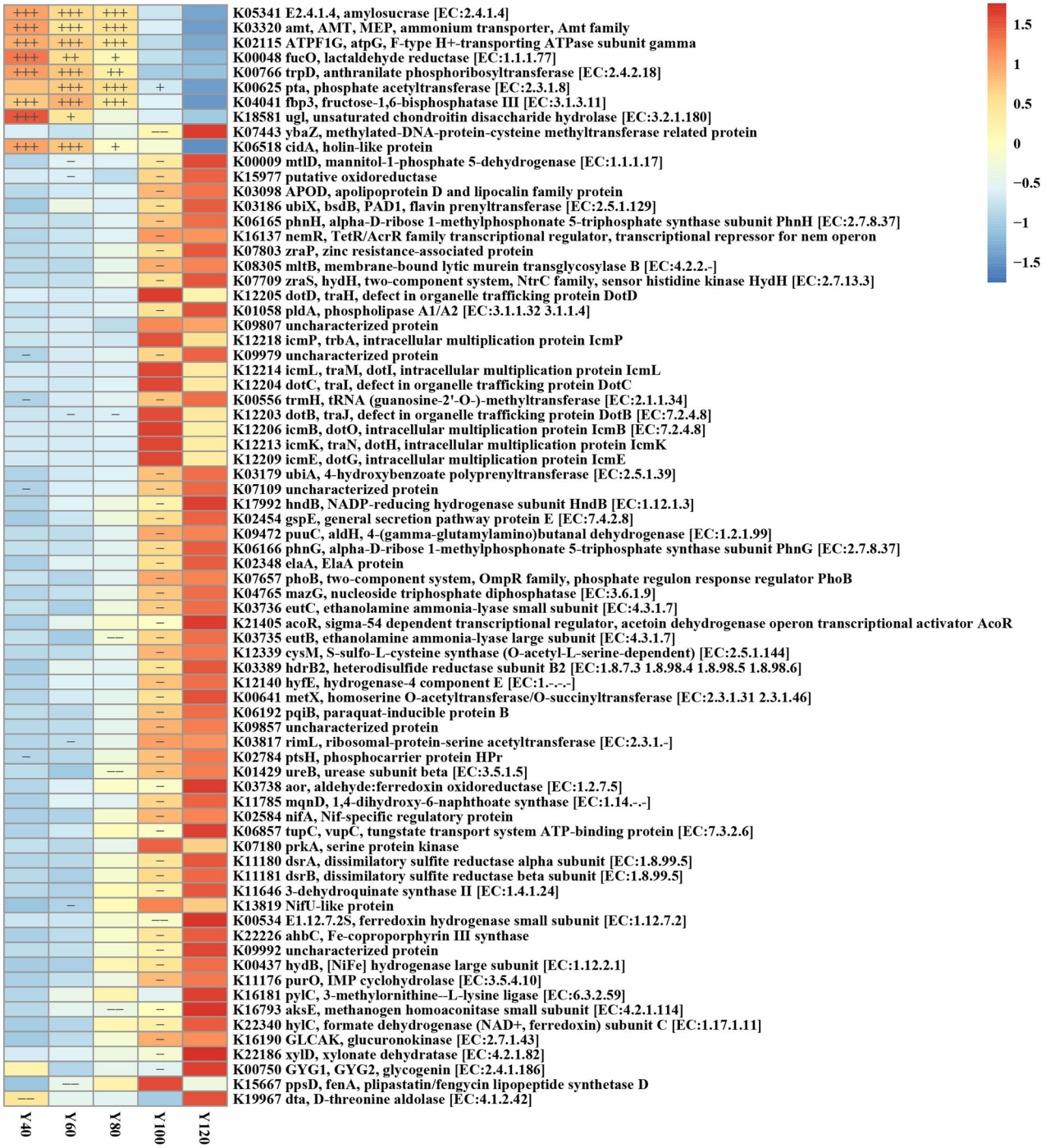

Fig. 4 | Changes of longevity-related bacterial genes in the KEGG pathway module and KO gene. Four stages (Y40, Y60, Y80, and Y100) showed significantly increased or decreased bacterial genes abundance compared with the centenarian group (Y120). Significant changes (increase or decrease) are shown as follows: +++, increased $P < 0.005$; ++, increased $P < 0.01$; +, increased $P < 0.05$; −−−, reduced $P < 0.005$; −−, decreased $P < 0.01$; and −, decreased $P < 0.05$.

Effects of metabolites of *L. plantarum* 124 (LP124) in aging mice

Previously, we targeted the isolation of *Lactobacillus* in the gut microbiota of a long-lived township population and screened and verified *Lactobacillus plantarum* 124 (LP124) with good anti-aging function through in vitro screening and in vivo verification methods. Metabolomics analysis showed that the serum levels of mesoconic acid (MA), lysine (Lys), and butyrate (But) in mice administered with LP124 were significantly higher than those in the model group[7]. To explore the potential anti-aging role of LP124, we studied the anti-inflammatory effects of MA, Lys, and But on the aging process in mice.

In terms of inflammatory factors (Fig. 6A), LP124, MA, Lys and But significantly decreased the levels of pro-inflammatory factors and significantly increased the levels of the anti-inflammatory factor. MA significantly reduced the levels of pro-inflammatory factors interleukin (IL)-1β, IL-6, IL-5, and tumour necrosis factor-alpha (TNF-α) in colon, liver, and kidney tissues, and significantly increased the levels of the anti-inflammatory factor IL-10 in these tissues. MA significantly decreased the levels of NOD-like receptor protein 3 (NLRP3), apoptosis-associated microprotein (ASC), and cysteine proteinase-1 (Casp-1) in colon, liver, and kidney tissues. In terms of oxidative stress (Fig. 6B), LP124, MA, and But

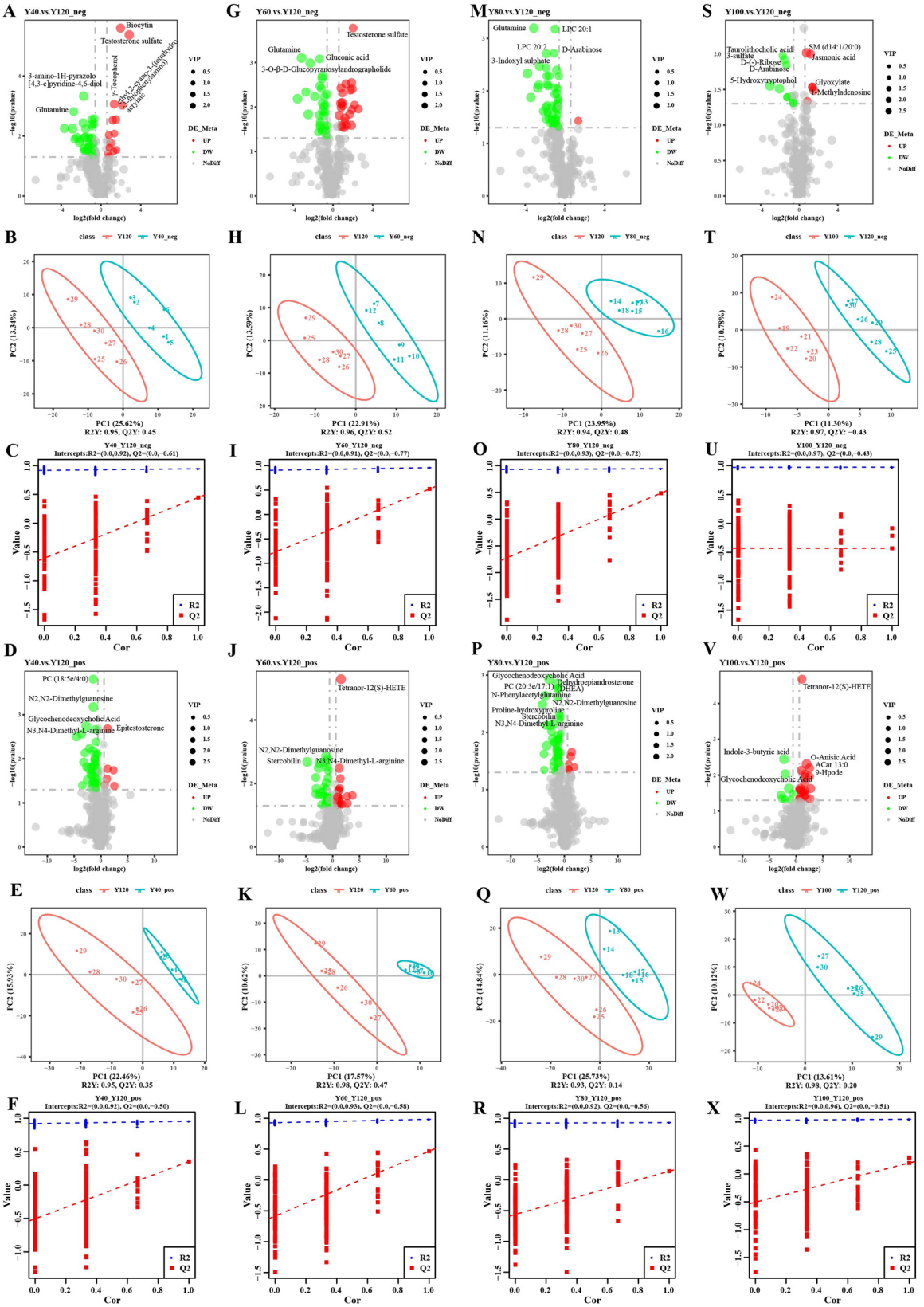

Fig. 5 | Characteristics of serum metabolites in the different age groups in Jiaoling. A–F Correlation diagram of different metabolite characteristics between the middle-aged (Y40) and centenarian (Y120) groups. **G–L** Correlation diagram of different metabolite characteristic analysis between the middle-aged group (Y60) and the centenarian group (Y120). **M–R** Correlation diagram for the analysis of differential metabolite characteristics between the older adult group (Y80) and the centenarian group (Y120). **S–X** Correlation graph for the analysis of differential metabolite characteristics between the older adult group (Y100) and the centenarian group (Y120). The metabolites labelled in the Fig. (**A**, **G**, **M**, **S** and **D**, **J**, **P**, **V**) setting a certain threshold of increase and decrease based on -log10 (p value) >3.0.

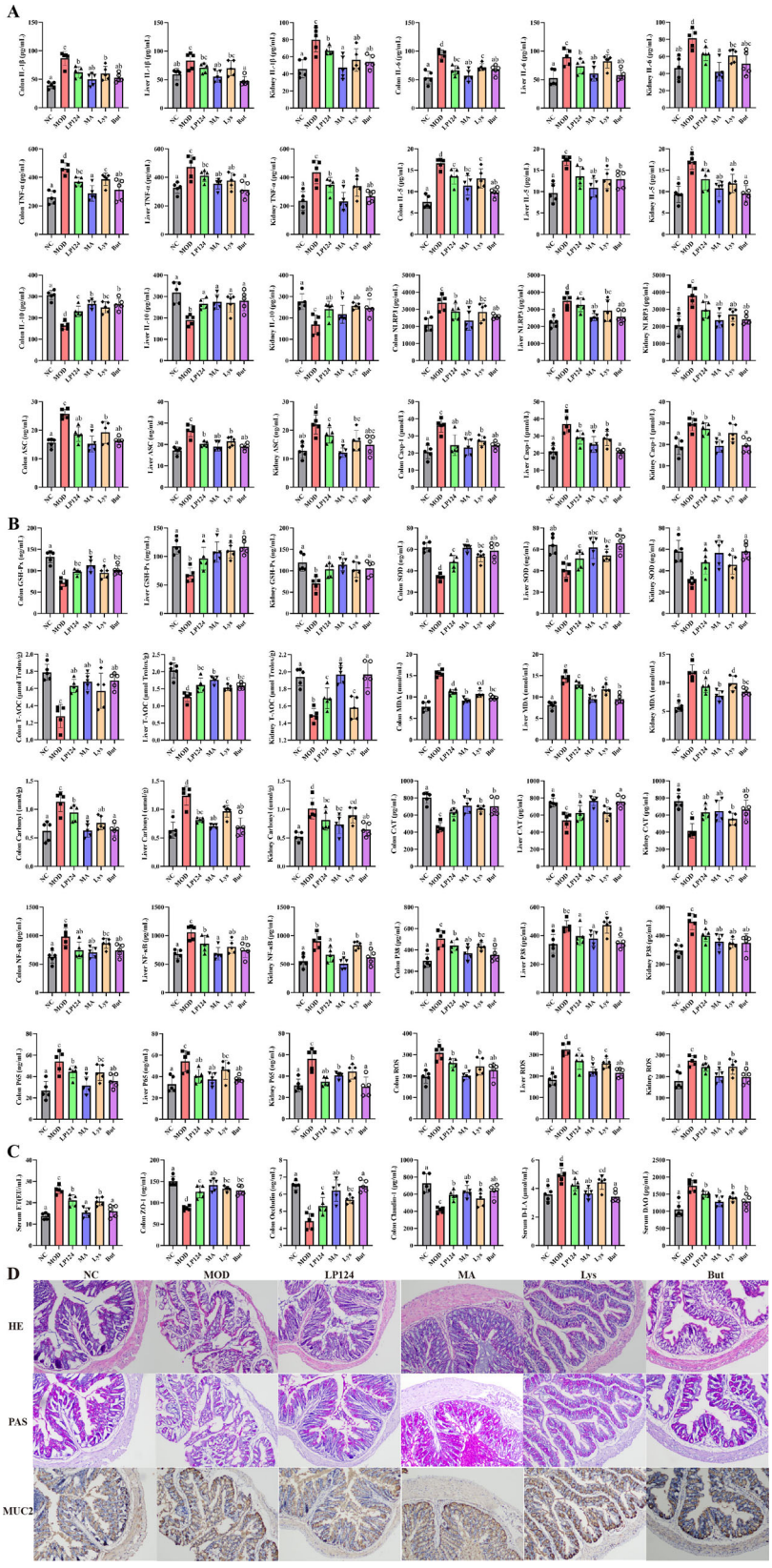

Fig. 6 | Effects of LP124, MA, Lys, and But in aging mice. Effects of LP124, MA, Lys, and But mesoconic acid, lysine, and butyrate on inflammatory factors (**A**), oxidative stress (**B**), intestinal barrier (**C**), haematoxylin and eosin (HE) staining, periodic acid-Schiff (PAS) staining, and immunohistochemistry of Mucin 2 (MUC2) in colonic tissue (**D**) in rapidly aging mice.

significantly increased the levels of glutathione peroxidase (GSH-Px), superoxide dismutase (SOD), total antioxidant (T-AOC), and catalase (CAT), and significantly reduced the levels of reactive oxygen species (ROS), malondialdehyde (MDA), carbonyl protein, nuclear factor kappa B (NF-κB), P38 protein, and P65 protein in colon, liver and kidney tissues. In terms of the intestinal barrier (Fig. 6C), LP124, MA, and Lys significantly increased the levels of zonula occludens protein 1 (ZO-1), tight junction protein (occludin), and claudin-1 in colon tissue. LP124, MA, and But significantly decreased the serum levels of d-lactic acid (D-LA), diamine oxidase (DAO), and endotoxin (ET). Hematoxylin and eosin staining revealed intact

intestinal mucosa in the LP124, MA, Lys, and But groups; the epithelial cells were arranged neatly; no exfoliated, necrotic, or inflammatory cell infiltration was observed; there were more scattered goblet cells between columnar cells; and no obvious abnormalities were observed in the structure of the muscle and serosal layers. Periodic acid-Schiff (PAS) staining was positive (PAS++) for the LP124, MA, and Lys groups. Immunohistochemistry was moderately positive for mucin 2 (MUC2++) (Fig. 6D).

The relative expression levels of mRNAs of the *GSH-Px*, *SOD*, thioredoxin reductase (*TrxR*), nuclear factor erythroid 2-related factor 2 (*Nrf2*), Kelch-like ECH-associated protein 1 (*Keap1*), B-cell leukaemia/lymphoma 2 protein (*Bcl2*), Bcl-2 associated X-protein (*Bax*), *NF-κB*, NOD-, LRR- and pyrin domain-containing protein 3 (*NLRP3*), and *Caspase-1* genes in colon tissues are shown in Supplementary Fig. 5A. LP124, MA, and Lys significantly increased the relative expression levels of *GSH-Px*, *SOD*, *TrxR*, and *Nrf2* mRNA, and significantly reduced the relative expression levels of *Bax* and *NLRP3* mRNA in colon tissues. LP124 and MA significantly reduced the relative mRNA expression levels of *Keap1*, *NF-κB*, and *Caspase-1* genes in colon tissue. MA significantly increased the relative expression of *Bcl2* mRNA in colon tissue. Finally, LP124 and MA significantly increased the level of nicotinamide adenine dinucleotide (NAD+) in the colon, liver, and kidney tissues (Supplementary Fig. 5B).

Regulation of MA, Lys, and But on the gut microbiota of aging mice

The α-diversity of mice gut microbiota was analysed. The results are provided in Supplementary Data 1. In terms of the abundance index, the observed species, Chao1, and Abundance Based Coverage Estimator (ACE) indices of the mouse gut microbiota were significantly increased by LP124, MA, Lys, and But group. In terms of the diversity index, LP124, MA, Lys, and But group significantly increased the Shannon index of the gut microbiota in mice. LP124, MA, Lys, and But group simultaneously increased the abundance of *Parabacteroides*, *Rikenellaceae* RC9 gut group, and *Bacteroides*, and simultaneously decreased the abundance of harmful bacteria *Helicobacter pylori*, *Escherichia–Shigella*, and *Staphylococcus* in the intestinal tract of mice. LP124 group increased the abundance of the beneficial bacteria *Akkermansia*, *Ruminococcus*, *Desulfovibrio*, *Oscillibacter*, *Alistipes*, and *Colidextribacter* in the intestines of mice. MA group increased the abundance of *Ligilactobacillus*, *Erysipelatoclostridium*, *Dubosiella*, *Parasutterella*, and *Haemophilus* in the intestinal tracts of the mice (Fig. 7A–F). Phylogenetic trees of the top 100 gut microbiota in mice at the genus level are shown in Supplementary Fig. 5C.

As shown in the histogram of the linear discriminant analysis (LDA) value distribution of the linear discriminant analysis effect size (LEfSe) analysis results of different species between NC, MOD, LP124, MA, Lys and But groups (Fig. 7G). NC group mainly contained the beneficial bacteria *Odoribacter*, *Alistipes*, and *Alloprevotella*. MOD group mainly harboured the harmful bacterium *Helicobacter*. LP124 group mainly contains the beneficial bacterium *Akkermansia*, and MA group mainly contains the butyricogenic bacteria *Dubosiella*. Lys group mainly contains *Bifidobacterium*; But group mainly contains *Bacteroides acidifaciens* and *Bacteroides sartorii* (Fig. 7G). In the statistical analysis, species with significant differences between groups at each classification level were identified using a t-test ($p < 0.05$). LP124, MA, Lys, and But group were significantly different from MOD group (Fig. 7H–K). The MA group contained *Bacteroides*, *Dubosiella*, *Parabacteroides*, and others (Fig. 7I).

Effects of MA, Lys, and But on serum metabolome of aging mice

Next, we analysed the LP124 metabolites in the serum metabolome of aging mice. In the LP124 vs. MOD comparison group, 248 positive mode metabolites were significantly different, of which 164 were upregulated and 84 were downregulated. A total of 123 negative mode metabolites exist with significant differences, of which 75 were upregulated and 48 were downregulated (Supplementary Fig. 6, Supplementary Data 2). The comparison revealed significantly upregulated metabolites, including taurochenodeoxycholic acid (sodium salt), taurocholic acid, tauroursodeoxycholic acid, and 3-hydroxybutyric acid (Supplementary Fig. 6A–F). A bubble diagram of KEGG enriched pathways for the LP124 vs. MOD comparison is shown in Supplementary Fig. 6G, H, and Supplementary Data 3 and 4. The results of the KEGG regulatory network analysis are provided in Supplementary Data 5 and 6. In the MA vs. MOD comparison, 260 positive mode metabolites were significantly different, among which 155 were upregulated and 105 were downregulated. A total of 131 negative mode metabolites were observed with significant differences, of which 61 were upregulated, and 70 were downregulated (Fig. 8, Supplementary Data 7). The MA vs. MOD comparison revealed significantly upregulated metabolites, including taurochenodeoxycholic acid (sodium salt), 3-hydroxybutyric acid, tauroursodeoxycholic acid, 7-ketolithocholic acid, and deoxycholic acid (Fig. 8A–F). A bubble diagram of KEGG enrichment data for MA vs. MOD is shown in Fig. 8G, H, and Supplementary Data 8 and 9. The KEGG regulatory network data for the MA vs. MOD comparison are provided in Supplementary Data 10 and 11.

In the Lys vs. MOD comparison group, 250 positive mode metabolites were significantly different, of which 152 were upregulated and 98 were downregulated. A total of 124 negative mode metabolites were observed with significant differences, of which 68 were upregulated and 56 were downregulated (Supplementary Fig. 7, Supplementary Data 12). A bubble diagram of KEGG enrichment data for Lys vs. MOD is shown in Supplementary Fig. 7G, H, and Supplementary Data 13 and 14. The KEGG regulatory network data for the Lys vs. MOD comparison are provided in Supplementary Data 15 and 16. In the But vs. MOD comparison group, 210 positive mode metabolites were significantly different, of which 128 were upregulated and 82 were downregulated. A total of 108 negative mode metabolites were observed with significant differences, of which 51 were upregulated, and 57 were downregulated (Supplementary Fig. 8, Supplementary Data 17). A bubble diagram of KEGG enrichment data for the But vs. MOD is shown in Supplementary Fig. 8G, H, and Supplementary Data 18 and 19. The KEGG regulatory network data for the But vs. MOD comparison are provided in Supplementary Data 20 and 21.

Analysis of the correlation among gut microbiota, metabolites, and physiological indicators of aging mice

We selected the top five differentially abundant bacteria at the genus level and compared the findings with the top ten differential metabolites to analyse the correlation between the gut microbiota and metabolites. The results of LP124, MA, Lys, and But vs. MOD are shown in Supplementary Fig. 9A–H, Supplementary Data 22–25. We selected the top 35 differentially prevalent bacteria genera and indicators, such as inflammatory factors, oxidative stress, and intestinal barrier, and analysed the correlation between the gut microbiota and physiological indicators (Supplementary Fig. 9I). Beneficial bacteria, including *Odoribacter*, *Alloprevotella*, *Parasutterella*, *Rikenellaceae* RC9 gut group, *Dubosiella*, *Alistipes*, *Bifidobacterium*, and *Haemophilus*, were significantly negatively correlated with pro-inflammatory factors IL-1β, IL-6, TNF-α, and NLRP3 inflammasome; pro-oxidation indices MDA, carbonyl, NF-κB, ROS, and ET; and intestinal barrier indices ZO-1, Claudin-1, DLA, and DAO. Positive correlations were evident for the anti-inflammatory factor IL-10 and the antioxidant factors SOD, T-AOC, and CAT. These bacteria have active anti-inflammatory roles. By contrast, *Lachnoclostridium* was significantly positively correlated with pro-inflammatory factors, inflammasomes, and pro-oxidation and intestinal barrier indices. This genus was negatively correlated with anti-inflammatory and antioxidant factors.

Discussion

The current cross-sectional analysis of a long-lived population cohort in Jiaoling, China, which is globally recognised for its long-lived residents, combined with metagenomics, metabolomics, and in vivo animal validation clarifies the gut microbiota characteristics and metabolic network of centenarians and verifies the key substance of anti-aging of the LP124 probiotic derived from centenarians (Fig. 9). Our results strongly suggest that the diversity of the gut microbiota in

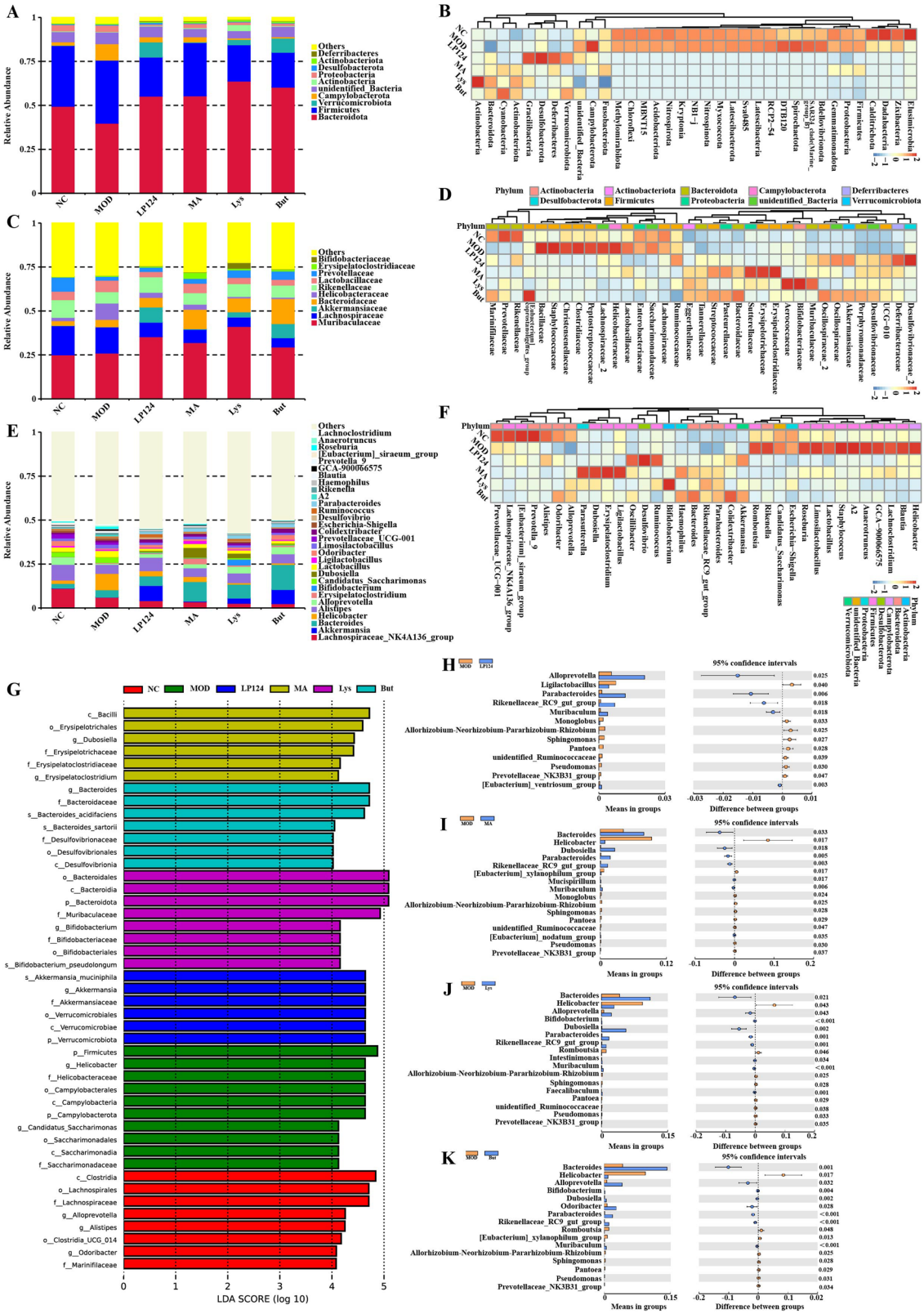

Fig. 7 | Regulatory effects of LP124, MA, Lys, and But on the gut microbiota of aging mice. Composition characteristics of the gut microbiota in mice at the phylum (**A**, **B**), family (**C**, **D**), and genus (**E**, **F**) levels. **G** LEfSe analysis of different species among the mouse gut microbiota under the NC, MOD, LP124, MA, Lys, and But conditions. T-test analysis of different species among mouse gut microbiota groups under LP124 (**H**), MA (**I**), Lys, (**J**), and But (**K**) conditions.

centenarians is significantly higher than that in young and middle-aged individuals, accompanied by the enrichment of beneficial symbiotic bacteria. These observations are similar to those of previous reports, which showed that, based on a variety of approaches, such as metabolomic capacity and gut microbiome diversity, centenarians have a gut microbiome associated with younger people, and their gut microbiome may be more similar to that of younger people[24,25]. Because the gut microbiome plays a key role in host health and

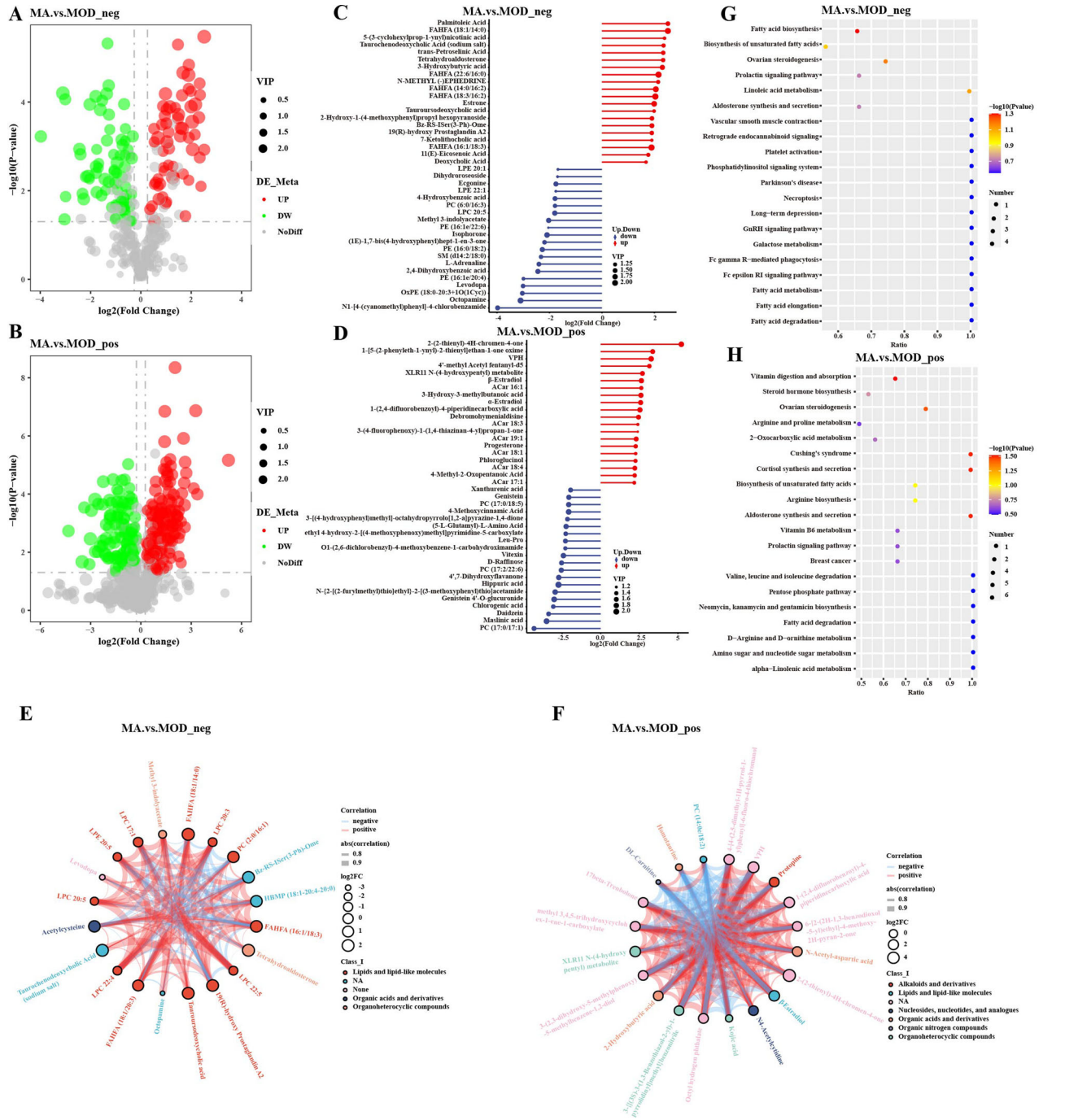

Fig. 8 | Effects of MA on serum metabolome of mice. A, **C** Volcano and differential metabolite chords of mouse serum metabolites in MA mice in negative mode. **B**, **D** Volcano and differential metabolite chords of serum metabolites in MA mice in the positive mode. Correlation between differential metabolites in MA mouse serum in the negative (**E**) and positive (**F**) mode. Bubble diagram of KEGG enrichment of MA mouse serum metabolites in negative (**G**) and positive (**H**) mode.

disease[26], we speculate that this unique gut microbiome profile and beneficial symbionts and their metabolites may contribute to longevity.

One of the main findings of this study is the significantly greater gut microbial diversity in centenarians compared to young and middle-aged adults. Consistent with these findings, a follow-up study on centenarians reported a consistently increased evenness of the gut microbiota[25]. In addition, consistent with observations in previous studies on older or younger adults, long-lived people with higher microbiome diversity tend to have fewer microbiome changes during aging, suggesting that greater diversity or species uniformity in centenarians compared to other older adults may protect the gut microbiota from instability[27,28]. The current findings show that, compared to young and middle-aged people, the gut microbiota of long-lived people was enriched with beneficial symbiotic bacteria, such as *Lactobacillus* and *Akkermannia*. Thus, preservation of beneficial symbiotic *Lactobacillus* may be a key feature associated with longevity. Several studies have reported that bacterial diversity decreases with age, and the colonisation of opportunistic pathogens (such as *Enterobacteriaceae*) increases. However, our study of the characteristics of the gut microbiota in centenarians during aging showed an increase in bacterial diversity and an increase in the abundance of the beneficial bacteria in the genus *Lactobacillus*. Several cross-sectional studies have shown that the composition of microbiota in centenarians plays an important role in

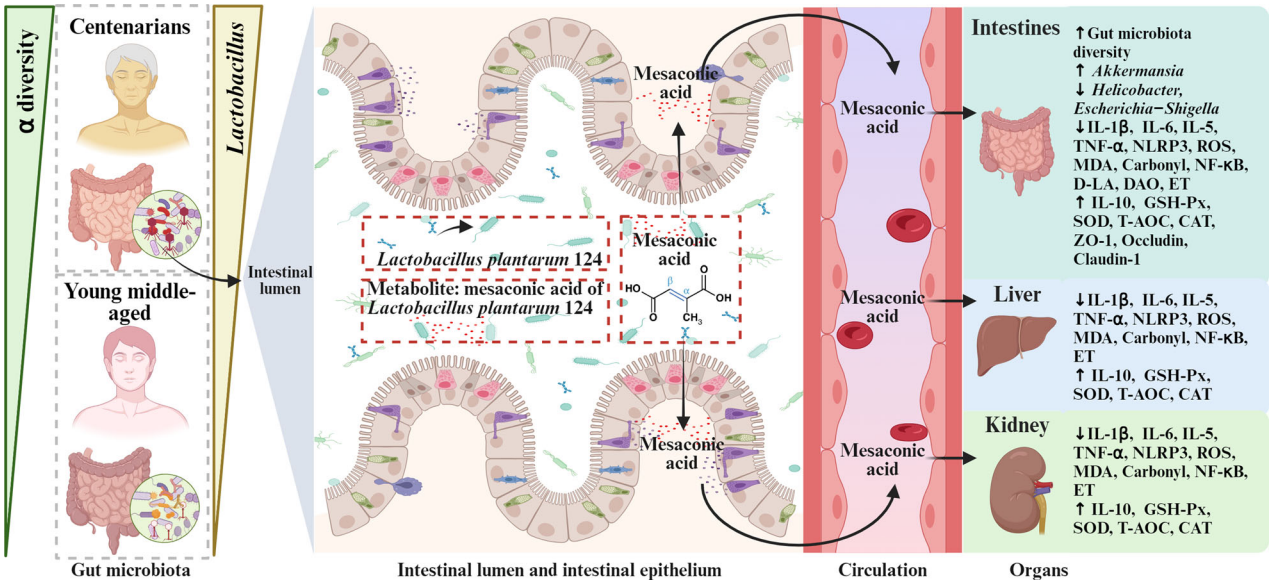

Fig. 9 | Anti-inflammation and anti-aging mechanisms of LP124 and mesaconic acid metabolite of LP124. Compared with young and middle-aged people, centenarians showed significantly increased α-diversity and *Lactobacillus* in the gut microbiota. Mesaconic acid from LP124 and centenarian metabolites have significant anti-inflammatory and anti-aging effects. Created using BioRender.com.

healthy aging. For example, Biagi et al. reported that in the centenarian group, the core microbiota composition was reduced and health-related bacteria (including *Akkermansia*, *Bifidobacterium*, and *Christensenella*) were enriched[17]. These findings are consistent with the results of our study. The enrichment of these beneficial microorganisms likely reflects the anti-aging pattern of gut microbiota in centenarians. Given that these bacteria typically secrete short-chain fatty acids and possess anti-inflammatory and antioxidant properties, their unique pattern of enrichment of beneficial microbes during aging may be associated with longevity.

Another major finding of this study from the metagenomic analysis results combined with the isolation, culture and screening in vitro was the identification of an LP124 strain with a good antioxidant effect. The basis of its anti-aging effect was explored through metagenomics, metabolomics, and experiments using rapidly aging mice. Finally, we confirmed that the MA metabolite of LP124 has potent, anti-inflammatory, and antioxidant effects. With the rapid development of second- and third-generation high-throughput sequencing technologies, most studies have been limited to metagenomic sequencing analysis of the gut microbiota. Most of these metagenomic sequencing results were not validated by further isolation of key strains for in vitro and in vivo experiments. For example, the gut microbiota structure of centenarians and young adults is reportedly highly similar[25], with a higher abundance of potentially beneficial *Bacteroides*, such as *Akkermansia*, in long-lived people[29]. In addition to a higher abundance of specific bacteria such as *Parabacteroides*, most bacteria have anti-inflammatory effects in their host[30]. The latter authors hypothesised that a healthy gut microbiota in centenarians promotes healthy aging. They posited that an underlying reason is increased chronic low-grade inflammation in the older adult, which is associated with various chronic diseases[31]. This is consistent with the results of this study. Coupled with the beneficial effects of these bacteria[32,33] and the lower susceptibility of centenarians to chronic diseases[34], these microbes might contribute to the health of centenarians[25]. However, these studies did not validate the results obtained through metagenomic analysis by further designing in vivo and in vitro experiments. The mechanisms underlying the enrichment of beneficial microorganisms in centenarians have not yet been fully elucidated.

In the present study, LP124 characterised by a good antioxidant effect was isolated and screened from the gut microbiota of centenarians. Animal experiments further verified that LP124 exerts anti-inflammatory effects related to MA, Lys, and But, which are the key substance for anti-aging. The MA metabolite of LP124 displayed the best anti-aging effect. MA, itaconic acid, and citriconic acid are isomers. Itaconic acid is an anti-inflammatory metabolite via activation of Nrf2 through the alkylation of KEAP1[35]. Citraconic acid inhibits aconitate decarboxylase 1 (immune responsive gene 1) catalysis, reduces interferon response and oxidative stress, and regulates inflammation and cell metabolism[36]. MA is synthesised from itaconic acid and plays an immunomodulatory role in macrophages[37]. This is consistent with our findings that MA had a significant anti-inflammatory effect, alleviated oxidative stress, and protected the intestinal barrier. In the current study, MA significantly increased the richness and diversity of the gut microbiota in aging mice and increased the abundance of butyricogenic bacteria in the genus *Dubosiella*. The collective findings indicate that MA regulates the gut microbiota, relieves inflammation and oxidative stress, and maintains the intestinal barrier. Our results are consistent with those of Zhang et al., who used intestinal faecal 16S rDNA sequencing and targeted metabolomics sequencing technology[38]. An important protective effect of the specific gut microbiota *Dubosiella* and its butyric acid metabolite in sepsis-associated brain injury has been discovered. The findings established the important role of gut microbiota in sepsis-associated brain injury and provided a basic research basis for targeted gut microbiota therapy in clinical practice[38]. The results of Cai et al., based on faecal metabolomics of healthy centenarians from a Chinese longevous region showed that longevity was closely related to beneficial metabolites such as phospholipids, amino acids and short-chain fatty acids (SCFAs)[39]. These provide guidance for the integration of multiomics techniques to identify aging and anti-aging biomarkers[40,41].

In conclusion, this study reports the composition and functional characteristics of gut microbiota in centenarians. Our results characterise a new metabolite strain with anti-inflammatory and anti-aging properties. The findings jointly highlight the positive role of the gut microbiota of long-lived people, especially the key intestinal symbiotic beneficial bacteria and their metabolites, which play an anti-aging role in health and longevity. The gut microbiota of centenarians is closely associated with longevity and is characterised by high species diversity and high levels of beneficial bacteria. Probiotics derived from the gut microbiota of centenarians, especially *Lactobacillus plantarum* 124 and its metabolite mesaconic acid, have a significant positive effect on health and longevity.

Methods

Ethics approval and study cohort

The overall purpose of this study was to use metagenomic and metabolomic methods to characterise the composition and function of the gut microbiota and serum metabolomics in different age groups in a township renowned for the longevity of its residents. The key strains were isolated, screened in vitro, and used in the senescence-accelerated mice (SAMR1 and SAMP8) to further explore the role of the key strains and their metabolites in the gut microbiota in health and longevity. This study was approved by the Ethics Committee (Ethics number: 2022(9)) of the First Affiliated Hospital of Guangdong Pharmaceutical University.

In total, 224 participants were randomly selected. All enroled participants signed an informed consent form before physical examination and biomaterial collection. Faecal samples were freshly collected from each subject and immediately frozen at −20 °C, transported to the laboratory on an ice pack, and stored in a −80 °C freezer until metagenomic analysis. Subsequently, serum samples were subjected to metabolomic analyses. For age-related group comparison analyses, we divided the participants from the Jiaoling cohort into middle-aged (Y40 and Y60, Y40: 21–40 years and Y60: 41–60 years), older adults (Y80 and Y100, Y80: 61–80 years and Y100: 81–99 years), and centenarian (Y120: 100–110 years) groups.

Metagenomic sequencing analysis

DNA was extracted from faecal samples, as previously described[42]. In this study, the Illumina HiSeq sequencing platform was used to obtain 11,619.54 Mbp of raw data. After quality control, an average of 11,604.59 Mbp was obtained. A mean of 219,259 open reading frames (ORFs) were obtained by gene prediction using MetaGeneMark software. The non-redundant gene set was compared with the MicroNR database using BLASTP, and species annotation was performed using the LCA algorithm. We used DIAMOND software[43,44] to perform common functional database annotations on non-redundant gene sets (e-value ≤ 10^{-5}). A total of 60.85% ORFs were compared to the KEGG database (Version 2018-01-01, http://www.kegg.jp/kegg/)[45,46], 59.72% were compared to the eggNOG database (Version 4.5, http://eggnogdb.embl.de/#/app/home)[47], and 3.09% were compared to the CAZy database (Version 20150704, http://www.cazy.org/)[48].

Analysis of composition characteristics of gut microbiota

The use of DIAMOND software[49] (v0.9.9.110, https://github.com/bbuchfink/diamond/), Link Unigenes to the NCBI NR database (Version 2018-01-02, https://www.ncbi.nlm.nih.gov/). For the comparison, the result of each sequence with e-value ≤ e-value*10^{50} was chosen. Since each sequence may have multiple comparison results, the LCA algorithm (applied to the systematic classification of MEGAN software[51] (https://en.wikipedia.org/wiki/Lowest_common_ancestor) to determine the sequence of species annotation information. The abundance of a species in a sample is equal to the sum of the annotated gene abundances of the species[52–54]. Starting from the abundance table at each classification level, Krona analysis[55] was performed, showing the general situation of relative abundance and the clustering heat map of abundance. Dimension reduction analysis was performed using PCA[56] (R ade4 package, Version 2.15.3) and NMDS[57] (R vegan package, Version 2.15.3).

Animal experiments and determination of biochemical index

The animal experiments were approved by the Institute of Microbiology, Guangdong Academy of Sciences (approval number: GT-IACUC202112281). SAMR1 and SAMP8 (SPF grade) mice obtained from Guangdong Jinzhihe Biotechnology Co., Ltd. (Guangdong, China) were housed under a 12-h light/dark cycle in gnotobiotic facilities. All mice were provided with sterile food and water ad libitum. Both the NC (SAMR1, 6 mice) and MOD (SAMP8, 6 mice) groups received 0.2 mL of normal saline by gavage daily. For the LP124 test group (SAMP8, 6 mice), 0.2 mL of LP124 suspension containing $1.0 \pm 0.05 \times 10^9$ colony forming units (CFU)/mL was administered[7]. For the MA test group (SAMP8, 6 mice), 0.2 mL of MA solution (200 mg/kg body weight/day) was administered. For the Lys test group (SAMP8, 6 mice), 0.2 mL of Lys solution (200 mg/kg body weight/day) was administered. For the But test group (SAMP8, 6 mice), 0.2 mL of But solution (200 mg/kg body weight/day) was administered. All administrations were by gavage daily for 9 weeks. The animals used in this experiment were anesthetized. The anaesthetic drug was sodium pentobarbital, which was administered by intraperitoneal injection. The injection dose was 40–50 mg/kg (2%) intraperitoneally. The principle was that sodium pentobarbital directly acted on the central nervous system through the blood circulation, inhibiting the activity of neurons, thereby achieving the anaesthetic effect. Colon, liver, and kidney tissue homogenates were prepared for analysis for pro-inflammatory factors IL-1β, IL-6, and TNF-α, and anti-inflammatory factors IL-10, NLRP3, ASC, and Casp-1 were measured using ELISA kits (Beijing winter song Boye Biotechnology Co. Ltd., Beijing, China). The oxidative stress markers GSH-Px, SOD, TrxR, T-AOC, MDA, CAT, carbonyl protein, NF-κB, and ROS were determined by detection kits (Nanjing Jiancheng Bio Co., Nanjing, China). Intestinal barrier factors ET, ZO-1, occludin, claudin-1, D-LA, and DAO were measured using an ELISA kit and a related detection kit (Beijing Winter Song Boye Biotechnology Co. Ltd.).

Morphological observations and immunohistochemical analysis

After the animals were euthanized, their colons were isolated. The tissues were fixed with 10% formalin, embedded in conventional paraffin, sectioned to a thickness of 4–5 μm, and observed using haematoxylin-eosin and PAS staining. MUC2 in the colon tissue was stained using immunohistochemistry. The intestinal morphology was observed and photographed using an inverted optical microscope.

Expression analysis of genes

Total RNA was extracted from the mouse colon using an RNeasy Mini Kit (Huangshi Yanke Biotechnology Co., Ltd., Hubei, China) according to the manufacturer's instructions. Quantitative RT-PCR was performed using SYBR Premix Ex Taq (Huangshi Yanke Biotechnology Co., Ltd., Hubei, China) on the 7500 Fast Real-Time PCR System (Applied Biosystems, Franklin Lakes, NJ, USA). The calculation of mRNA expression was performed by the $2^{-\Delta\Delta CT}$ method using the geometric mean of the housekeeping genes *GSH-Px*, *SOD*, *TrxR*, *Nrf2*, *Keap 1*, *Bax*, *Bcl 2*, *NF-κB*, *NLRP3*, and *Caspase 1*. Gene and primer sequences are listed in Supplementary Data 26. Comparisons between groups were performed using a one-way analysis of variance with $n = 6$ per group. All results are expressed as mean ± SD of the biological replicates.

Mass spectrometry

Serum samples were collected from people in the different age groups (Supplementary Data 27–29), and the NC, MOD, LP124, MA, Lys, and But groups ($n = 6$ per group) (Supplementary Data 30, 31). Acetonitrile was used to extract metabolites by protein precipitation. Untargeted metabolomic profiling was performed using liquid chromatography coupled with a High-Field Qexactive mass spectrometer (Thermo Fisher Scientific, Waltham, MA, USA; HILIC/ESI+, C18/ESI−, 85–1275 m/z, 120k resolution). Spectral features (m/z, retention time) corresponding to the identified and uncharacterized metabolites were integrated and aligned using apLCMS/xMSanalyzer software. MetaboAnalyst[58] was used for statistical analysis, and Mummichog software[59] was used for pathway enrichment analysis and verified by retention time, m/z, and tandem mass spectrometry using authenticated standards. Candidate molecules were identified following ion dissociation experiments on a Thermo Scientific Fusion mass spectrometer, and the spectral library was matched to the mzCloud, mzVault, and MassList libraries using Compound Discoverer 3.0.

Statistical analyses

According to the different data, statistical analyses between groups were performed using Wilcoxon's rank sum test, Student's *t* test, or one-way ANOVA. Results are expressed as mean ± SD. Statistical analyses and data

visualisation were performed using the R software (v2.15.3) with the WGCNA, stats, and ggplot2 software packages.

Data availability

The sequence data for all samples have been deposited in the NCBI Sequence Read Archive (SRA) under accession code BIOProject: PRJNA895352. Other data that support the findings of this study are available within the paper and its Supplementary Information files or from the corresponding author upon reasonable request.

Received: 9 December 2024; Accepted: 8 August 2025;
Published online: 19 August 2025

References

1. Cani, P. D. Human gut microbiome: hopes, threats and promises. *Gut* **67**, 1716–1725 (2018).
2. de Vos, W. M., Tilg, H., Van Hul, M. & Cani, P. D. Gut microbiome and health: mechanistic insights. *Gut* **71**, 1020–1032 (2022).
3. Kim, S. & Jazwinski, S. M. The gut microbiota and healthy aging: a mini-review. *Gerontology* **64**, 513–520 (2018).
4. Yatsunenko, T. et al. Human gut microbiome viewed across age and geography. *Nature* **486**, 222–227 (2012).
5. DeJong, E. N., Surette, M. G. & Bowdish, D. M. E. The gut microbiota and unhealthy aging: disentangling cause from consequence. *Cell Host Microbe* **28**, 180–189 (2020).
6. Peterson, C. T., Sharma, V., Elmen, L. & Peterson, S. N. Immune homeostasis,dysbiosisand therapeutic modulationofthegutmicrobiota. *Pharmacol. Therapeutics* **179**, 363–377 (2015).
7. Wu, L. et al. Gut microbiota as an antioxidant system in centenarians associated with high antioxidant activities of gut-resident *Lactobacillus*. *npj Biofilms Microbiomes* **8**, 102 (2022).
8. Ghosh, T. S., Shanahan, F. & O' Toole, P. W. The gut microbiome as a modulator of healthy ageing. *Nat. Rev. Gastroenterol. Hepatol.* **19**, 565–584 (2022).
9. Li, H. J., Qi, Y. Y. & Jasper, H. Preventing age-related declineof gut compartmentalization limits microbiota dysbiosisand extends lifespan. *Cell Host Microbe* **19**, 240–253 (2016).
10. Wilmanski, T. et al. Gut microbiome pattern reflects healthy ageing and predicts survival in humans. *Nat. Metab.* **3**, 274–286 (2021).
11. Larson, P. J. et al. Associations of the skin, oral and gut microbiome with aging, frailty and infection risk reservoirs in older adults. *Nat. Aging* **2**, 941–955 (2022).
12. Wu, L. et al. Washed microbiota transplantation improves patients with metabolic syndrome in South China. *Front. Cell. Infect. Microbiol.* **12**, 1044957 (2022).
13. Wu, L. et al. Washed microbiota transplantation improves patients with high blood glucose in South China. *Front. Endocrinol.* **13**, 985636 (2022).
14. Wu, L. et al. Washed microbiota transplantation improves patients with overweight by the gut microbiota and sphingolipid metabolism. *Biomedicines* **11**, 2415 (2023).
15. Claesson, M. J. et al. Gut microbiota composition correlates with diet and health in the elderly. *Nature* **488**, 178–184 (2012).
16. Kim, B.-S. et al. Comparison of the gut microbiota of centenarians in longevity villages of South Korea with those of other age groups. *J. Microbiol. Biotechnol.* **29**, 429–440 (2019).
17. Biagi, E. et al. Gut microbiota and extreme longevity. *Curr. Biol.* **26**, 1480–1485 (2016).
18. Sato, Y. et al. Novel bile acid biosynthetic pathways are enriched in the microbiome of centenarians. *Nature* **599**, 458–464 (2021).
19. Rampelli, S. et al. Shotgun metagenomics of gut microbiota in humans with up to extreme longevity and the increasing role of xenobiotic degradation. *mSystems* **5**, e00124-20 (2020).
20. Wu, L. et al. A cross-sectional study of compositional and functional profiles of gut microbiota in Sardinian centenarians. *mSystems* **4**, e00325-19 (2019).
21. Tavella, T. et al. Elevated gut microbiome abundance of Christensenellaceae, Porphyromonadaceae and Rikenellaceae is associated with reduced visceral adipose tissue and healthier metabolic profile in Italian elderly. *Gut Microbes* **13**, 1–19 (2021).
22. Ren, M., Li, H., Fu, Z. & Li, Q. Succession analysis of gut microbiota structure of participants from long-lived families in Hechi, Guangxi, China. *Microorganisms* **9**, 2524 (2021).
23. Zhang, S. et al. Gut microbiota in healthy and unhealthy long-living people. *Gene* **779**, 145510 (2021).
24. Kong, F., Deng, F., Li, Y. & Zhao, J. Identification of gut microbiome signatures associated with longevity provides a promising modulation target for healthy aging. *Gut Microbes* **10**, 210–215 (2019).
25. Pang, S. et al. Longevity of centenarians is reflected by the gut microbiome with youth-associated signatures. *Nat. Aging* **3**, 436–449 (2023).
26. Biagi, E. et al. The gut microbiota of centenarians: signatures of longevity in the gut microbiota profile. *Mech. Ageing Dev.* **165**, 180–184 (2017).
27. Chen, L. et al. The long-term genetic stability and individual specificity of the human gut microbiome. *Cell* **184**, 2302–2315 (2021).
28. Jeffery, I. B., Lynch, D. B. & O'Toole, P. W. Composition and temporal stability of the gut microbiota in older persons. *ISME J.* **10**, 170–182 (2016).
29. Raftar, S. K. A. et al. The anti-inflammatory effects of Akkermansia muciniphila and its derivates in HFD/CCL4-induced murine model of liver injury. *Sci. Rep.* **12**, 2453 (2022).
30. Hiippala, K. et al. Isolation of anti-inflammatory and epithelium reinforcing Bacteroides and Parabacteroides spp. from a healthy fecal donor. *Nutrients* **12**, 935 (2020).
31. Deng, F., Li, Y. & Zhao, J. The gut microbiome of healthy long-living people. *Aging* **11**, 289–290 (2019).
32. Cani, P. D. & Knauf, C. A newly identified protein from Akkermansia muciniphila stimulates GLP-1 secretion. *Cell Metab.* **33**, 1073–1075 (2021).
33. Zafar, H. & Saier, M. H. Jr Gut species in health and disease. *Gut Microbes* **13**, 1–20 (2021).
34. Hirata, T. Associations of cardiovascular biomarkers and plasma albumin with exceptional survival to the highest ages. *Nat. Commun.* **11**, 3820 (2020).
35. Mills, E. L. et al. Itaconate is an anti-inflammatory metabolite that activates Nrf2 via alkylation of KEAP1. *Nature* **556**, 113–117 (2018).
36. Chen, F. et al. Citraconate inhibits ACOD1 (IRG1) catalysis, reduces interferon responses and oxidative stress, and modulates inflammation and cell metabolism. *Nat. Metab.* **4**, 534–546 (2022).
37. He, W. et al. Mesaconate is synthesized from itaconate and exerts immunomodulatory effects in macrophages. *Nat. Metab. 2022* **4**, 524–533 (2022).
38. Zhang, H. et al. Gut microbiota mediates the susceptibility of mice to sepsis-associated encephalopathy by butyric acid. *J. Inflamm. Res.***15**, 2103–2119 (2022).
39. Cai, D. et al. The age-accompanied and diet-associated remodeling of the phospholipid, amino acid, and SCFA metabolism of healthy centenarians from a Chinese longevous region: a window into exceptional longevity. *Nutrients* **14**, 4420 (2022).
40. Wu, L. et al. Metagenomics-Based Analysis Of The Age-related Cumulative Effect Of Antibiotic Resistance Genes In Gut Microbiota. *Antibiotics* **10**, 1006 (2021).
41. Wu, L. et al. Integrated multi-omics for novel aging biomarkers and antiaging targets. *Biomolecules* **12**, 39 (2021).
42. Qin, J. et al. A metagenome-wide association study of gut microbiota in type 2 diabetes. *Nature* **490**, 55–60 (2012).

43. Feng, Q. et al. Gut microbiome development along the colorectal adenoma-carcinoma sequence. *Nat. Commun.* **6**, 6528 (2015).
44. Li, J. et al. An integrated catalog of reference genes in the human gut microbiome. *Nat. Biotechnol.* **32**, 834–841 (2014).
45. Kanehisa, M. et al. From genomics to chemical genomics: new developments in KEGG. *Nucleic Acids Res.* **34**, D354–D357 (2006).
46. Kanehisa, M. et al. KEGG: new perspectives on genomes, pathways, diseases and drugs. *Nucleic Acids Res.* **45**, D353–D361 (2017).
47. Jaime, H. C. et al. eggNOG 4.5: a hierarchical orthology framework with improved functional annotations for eukaryotic, prokaryotic and viral sequences. *Nucleic Acids Res.* **44**, D286–D293 (2016).
48. Schiebenhoefer, H. et al. A complete and flexible workflow for metaproteomics data analysis based on MetaProteomeAnalyzer and Prophane. *Nat. Protoc.* **15**, 3212–3239 (2020).
49. Buchfink, B., Xie, C. & Huson, D. H. Fast and sensitive protein alignment using DIAMOND. *Nat. Methods* **12**, 59–60 (2015).
50. Oh, J. et al. Biogeography and individuality shape function in the human skin metagenome. *Nature* **514**, 59–64 (2014).
51. Huson, D. H. et al. Integrative analysis of environmental sequences using MEGAN4. *Genome Res.* **21**, 1552–1560 (2011).
52. Karlsson, F. H. et al. Gut metagenome in European women with normal, impaired and diabetic glucose control. *Nature* **498**, 99–103 (2013).
53. Karlsson, F. H. et al. Symptomatic atherosclerosis is associated with an altered gut metagenome. *Nat. Commun.* **3**, 1245 (2012).
54. Qin, J. et al. A human gut microbial gene catalogue established by metagenomic sequencing. *Nature* **464**, 59–65 (2010).
55. Ondov, B. D., Bergman, N. H. & Phillippy, A. M. Interactive metagenomic visualization in a Web browser. *BMC Bioinforma.* **12**, 385 (2011).
56. Avershina, E., Frisli, T. & Rudi, K. De novo semi-alignment of 16S rRNA gene sequences for deep phylogenetic characterization of next generation sequencing data. *Microbes Environ.* **28**, 211–216 (2013).
57. Rivas, M. N. et al. A microbiota signature associated with experimental food allergy promotes allergic sensitization and anaphylaxis. *J. Allergy Clin. Immunol.* **131**, 201–212 (2013).
58. Xia, J. & Wishart, D. S. Using MetaboAnalyst 3.0 for comprehensive metabolomics data analysis. *Curr. Protoc. Bioinforma.* **55**, 14.10.1–14.10.91 (2016).
59. Li, S. et al. Predicting network activity from high throughput metabolomics. *PLoS Comput. Biol.* **9**, e1003123 (2013).

Acknowledgements

This study was supported by the Key-Area Research and Development Program of Guangdong Province (No. 2022B1111070006), the Basic and Applied Basic Research Fund of Guangdong Province (No. 2025A1515011113, No. 2023A1515012578), the China postdoctoral science foundation (No. 2023M740782), Guangdong Province Young Innovative Talents Funds (No. 2023KQNCX029), College Student Inovation and Entrepreneurship Training Program Project (No. S202311347045) and Excellent Doctoral Talent Program for the Zhongkai University of Agriculture and Engineering (No. KA23YY318A5). We would like to thank all those who participated in the studies, in particular our study subjects and Beijing Novogene Technology Co., Ltd.

Author contributions

Q.W., X.H., X.X., and L.W. conceived and designed this study. L.W., H.H., T.L., G.D., L.L. Y.L. J.Z., N.C., T.J., J.Y., H.Z., Q.G., and H.G. assembled the cohorts, collected the specimens and biological data. H.Z. oversaw the transfer of specimens and clinical metadata and provided clinical insights. L.W., H.H. and G.L. performed faecal samples culturing experiments and isolate genomic DNA extraction. L.W. were in charge of animal experiments. L.W., H.H., T.L., G.D., L.L., H.Z., J.W., S.F., S.L., G.L., W.X., and L.W. analysed clinical metadata, shotgun metagenomic sequencing data, isolate genome sequencing data and functional metagenomic data. L.W. drafted the manuscript. Q.W., X.H., X.X., and L.W. revised the manuscript. Q.W., X.H. and X.X. supervised the project. L.W., H.H., T.L., G.D. L.L., and H.Z. contributed equally. All authors approved the final version of the manuscript.

Competing interests

The authors declare no competing interests.

Additional information

Supplementary information The online version contains supplementary material available at https://doi.org/10.1038/s41522-025-00812-9.

Correspondence and requests for materials should be addressed to Qingping Wu, Xinqiang Xie or Xingxiang He.